# Enhancing Explainability and Reliable Decision-Making in Particle Swarm Optimization through Communication Topologies

Nitin Gupta
Department of Mathematics and
Computing
Dr BR Ambedkar NIT Jalandhar
Jalandhar, India
niting.ma.23@nitj.ac.in

Indu Bala
University of Adelaide
Adelaide, Australia
indu.bala@adelaide.edu.au

Bapi Dutta
University of Jaén
Jaén, Spain
bdutta@ujaen.es

Luis Martínez
University of Jaén
Jaén, Spain
martin@ujaen.es

Anupam Yadav*
Department of Mathematics and
Computing
Dr BR Ambedkar NIT Jalandhar
Jalandhar, India
anupam@nitj.ac.in

## Abstract

Swarm intelligence effectively optimizes complex systems across fields like engineering and healthcare, yet algorithm solutions often suffer from low reliability due to unclear configurations and hyper-parameters. This study analyzes Particle Swarm Optimization (PSO), focusing on how different communication topologies—Ring, Star, and Von Neumann—affect convergence and search behaviors. Using an adapted IOHxplainer, an explainable benchmarking tool, we investigate how these topologies influence information flow, diversity, and convergence speed, clarifying the balance between exploration and exploitation. Through visualization and statistical analysis, the research enhances interpretability of PSO's decisions and provides practical guidelines for choosing suitable topologies for specific optimization tasks. Ultimately, this contributes to making swarm-based optimization more transparent, robust, and trustworthy.

## CCS Concepts

• **Computing methodologies** → *Search methodologies*; **Meta-heuristics**; **Explainable AI**.

## 1 Introduction

The efficacy of PSO [7] is significantly influenced by its communication topology—the schematic arrangement that dictates how individual solutions, termed 'particles', share information. This architecture is critical as it directly impacts the swarm's ability to efficiently explore and exploit the search space, thus affecting overall algorithm performance [9]. Traditional topologies such as Ring, Star, and Von Neumann offer distinct dynamics that can either hinder or enhance the swarm's optimization capabilities. Moreover, advancements in PSO have focused on augmenting its core strategies to overcome challenges such as premature convergence to local optima and enhancing its adaptability through methods like hybridization and strategic parameter adjustments [6].

Even with progress, PSO still runs into issues because it works like a "black box," leaving its decision-making unclear. This lack of clarity can make it hard to build trust and verify outcomes, especially in important areas like healthcare and self-driving systems. To tackle this problem, Explainable Artificial Intelligence (XAI) [2] has come into play as a helpful way to make complicated algorithms easier to understand and more accountable. In this work, we aim to enhance the explainability and trustworthiness of PSO by exploring its dynamics under different communication topologies. Our objectives are to

(1) Analyze how various topologies influence the search efficacy and convergence behaviors of PSO.
(2) Employ XAI methodologies to provide insights into the decision-making processes of PSO, enhancing the explainability and trustworthiness of the optimization results.
(3) Evaluate the performance of PSO under each topology using benchmark functions to determine optimal configurations for different types of optimization problems.

## 2 Methodology

Explainable Artificial Intelligence (XAI) is becoming increasingly crucial in AI and machine learning. It enhances the transparency, trustworthiness, and interpretability of AI models, which is essential as these models progressively affect more areas of everyday life and critical decision-making. It helps clarify how these algorithms process and behave during search operations, which often involve intricate interactions and adjustments [1]. Utilizing XAI techniques

enables both researchers and practitioners to uncover how various algorithm components affect overall performance, observe how solutions develop over time, and understand the factors that drive algorithms towards optimal solutions.

## 2.1 Particle Swarm Optimization (PSO)

PSO [7] optimizes an objective function by refining candidate solutions iteratively. Each "particle" represents a potential solution, and its position is updated based on its experience and its neighbors' positions.

$$v_i(t + 1) = wv_i(t) + c_1r_1(p_{best,i} - x_i(t)) + c_2r_2(g_{best} - x_i(t)) \quad (1)$$

$$x_i(t + 1) = x_i(t) + v_i(t + 1) \quad (2)$$

Equations 1 and 2 are the velocity and position update in PSO. Here, $v_i(t)$ and $x_i(t)$ are the velocity and current position of particle $i$ at time $t$, other parameters having their standard definitions as mentioned in Table 1.

In this research, we consider three topologies: Ring, Star, and Von-Neumann, and analyze their configurations for better explainability. In the Star topology, each particle is influenced by the best known position globally [12, 13]. In Ring topology, each particle shares information with its $k$ nearest neighbors, encouraging diversity and exploration [9, 14]. In Von Neumann topology, particles are connected in a grid, with communication based on Delannoy numbers, promoting structure [11, 15].

## 2.2 Explainer Framework for Swarm Intelligence

In this work, we adapted the IOHxplainer framework to analyze PSO behavior across hybrid topologies, enhancing it with XAI methods to assess the impact of different configurations. The framework supports continuous, integer, and categorical parameters—similar to SMAC [3, 8]—and accounts for hyper-parameter dependencies for detailed PSO configuration.

Experiments use either grid or stochastic sampling methods, with an evaluation budget for each PSO configuration tested against the Black-Box Optimization Benchmark (BBOB) [5], which includes 24 noiseless functions in the COCO framework [4]. SHAP-based XAI methods [10] are used to determine the marginal impact of each parameter on PSO's performance, aiding in the interpretability of the results.

This is usually done with a swarm plot, giving PSO designers and users a clear picture of how different hyperparameters affect performance in various situations and across different setups.

To use the IOHxplainer in swarm intelligence studies, we start with a phase dedicated to gathering data, which might involve large grids or random samples of configurations. You can find a more detailed explanation of the framework in Figure 1. The results are summarized in the following sections and can also be found on this GitHub link: https://github.com/GitNitin02/ioh_pso.

## 3 Experiment Setups and Result Discussion

This section details the experimental setup and configuration of PSO and its associated topologies, focusing on its explainability through the explainable framework. For comprehensive evaluation, we apply this framework to a diverse set of benchmark functions.

**Table 1: PSO module and their configurable hyperparameter for each topologies for d=2.**

| Hyperparameter | Shorthand | Domain |
|---|---|---|
| Cognitive coefficient | $c_1$ | {0.3, 0.5, 0.7, 0.9} |
| Social coefficient | $c_2$ | {0.2, 0.4, 0.6, 0.7} |
| Inertia weight | $w$ | {0.9, 1.2, 0.4} |
| Number of particles | $n$ | {50, 100, 150} |
| Nearest $k$ neighbors | $k$ | {1, 2, 3} |
| Minkowski $p$-norm | $p$ | {1, 2} |
| Delannoy numbers | $r$ | {1, 2} |

The BBOB functions include a combination of unimodal, multimodal, and highly multimodal functions. Functions f1, f2, f5 to f14 are unimodal, f3, f4, f15, f16, f20, f23, and f24 are multimodal, and f17, f18, f19, f21, and f22 are highly multimodal.

We obtain results on all 24 BBOB functions in 2 d for every configuration we examine, with a budget of 100 iterations in Star, Ring and Von Neumann topologies. Table 1 presents the basic configuration of PSO with respect to each topology for 2 d. Each function's initial five instances are used, and each instance is run five times independently. The normalized Area Over the Convergence Curve (AOCC 3) is a performance metric used to evaluate the efficiency of optimization algorithms and is defined as:

$$AOCC(\bar{y}) = \frac{1}{B} \sum_{i=1}^{B} \left( 1 - \frac{min(max((yi), lb), ub) - lb}{ub - lb} \right) \quad (3)$$

Here, $\bar{y}$ is the series of optimal function values found so far, $B$ is the budget, and $lb$ and $ub$ are the lower and upper bounds of the function value range. Empirical cumulative distribution function (ECDF) is a statistical tool used for distribution of data. AOCC is the area under the ECDF curve with infinite targets inside the limits. Prior to computing AOCC, function values are log-scaled in accordance with BBOB rules [5], with limitations of -5 and 5 for the 2 d functions. These experiments are conducted using standard computational resources: Intel i7 CPU, 32 GB RAM, 8 cores.

## 4 Contribution of Hyperparameters

We examine 1,728 PSO configurations across 24 BBOB functions, focusing on the impact of different communication topologies and hyperparameters on performance. Using SHAP-based plots for 2 d (Table 1), we analyze the contribution parameters such as n_particles, $c_1$, $c_2$, $p$ etc. to the optimization. The SHAP values indicate how each parameter affects the AOCC, with yellow dots representing positive contributions and violet dots indicating negative ones. Notably, a lower $c_1$ value consistently improves performance, while a larger $c_1$ worsens it. For unimodal functions, a smaller n_particle(50) performs best in a ring topology, while for multimodal functions, a larger value (100) works better. In contrast, the star topology benefits from a smaller n_particle for highly multimodal functions.

Higher SHAP values correlate with better accuracy. In Figure 2, for the Star topology, the unimodal function (f1) shows yellow dots
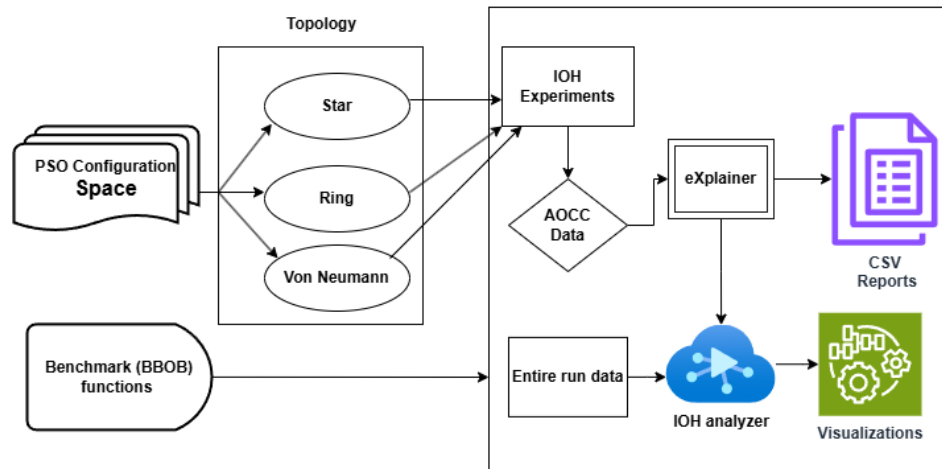
**Figure 1: The proposed framework for PSO configuration for automate and explainable analysis.**
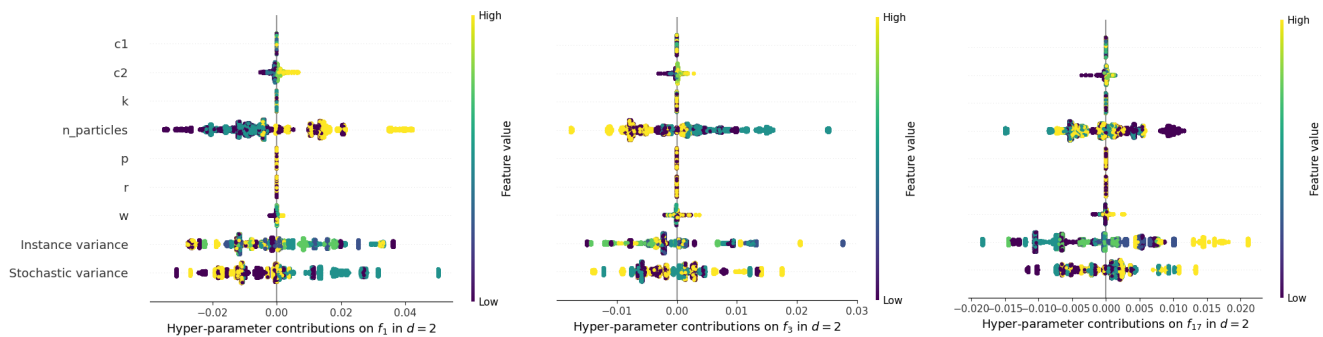


**Figure 2: Hyper-parameter contributions per benchmark function for d=2 for PSO using Star Topology.**

on the positive side of n_particles, indicating improved accuracy. The multi-modal function (f17) displays blue dots, suggesting that higher values reduce accuracy. Green dots on the positive side of the multimodal function (f3) indicate a moderate SHAP value with a modest accuracy impact.

## 4.1 Algorithm/configuration selection

In this experiment, we computed the "single-best" and "avg-best" configurations for each topology—Star, Ring, and Von Neumann. We identified the best configuration per BBOB function ("single-best mean") and the best overall ("avg-best mean"), comparing them with average performance and standard deviations. As shown in Table 2, PSO performs well on unimodal and simpler multimodal functions, showing low variance and stable convergence. However, it struggles on complex multimodal functions, particularly under the Star topology, due to poor escape from local optima. Functions like f3, f5, and f9 show strong performance. The Ring topology improves exploration through localized information sharing but converges slower and remains challenged on difficult landscapes. Full results are provided in the repository made available on https://github.com/GitNitin02/ioh_pso.

Due to space constraints, refer to the provided GitHub link for detailed experiment results. Based on Table 2 settings, the Ring topology outperforms the Von Neumann and Star topologies in terms of the $R^2$ value, which typically indicates a better fit for regression tasks. While the Star topology shows a higher mean, the Ring topology is the superior choice for regression tasks focused on maximizing the $R^2$ value. Our analysis shows that the Von Neumann topology is the most time-efficient for PSO, taking 6.56 hours to run all 24 functions at dimension 2. The Star topology takes 7.2 hours, and the Ring topology takes 9.35 hours. Von Neumann's efficiency is due to its structured communication, while the Ring topology's higher time complexity is likely due to its sequential neighbor-based exchange. This highlights the impact of topology on PSO's computational cost and efficiency.

## 5 Conclusion:

This research advances the explainability of PSO by investigating how different communication topologies affect its performance. Using a modified IOHxplainer framework, we evaluated 24 benchmark functions with multiple instances and seeds. Our findings reveal that Von Neumann topology enhances diversity and gradual convergence, making it suitable for complex optimization landscapes. Ring

**Table 2: Performance of Star, Ring and Von Neumann Topologies over all BBOB functions.**

| Function | Topologies | single-best mean | single-best std | avg-best mean | avg-best std | all mean | all std | R2 train |
|---|---|---|---|---|---|---|---|---|
| f1 | Star | 2.50E-01 | 5.40E-02 | 2.23E-01 | 2.62E-02 | **2.34E-01** | 4.18E-02 | 9.76E-01 |
|  | Ring | 2.50E-01 | 5.40E-02 | 2.23E-01 | 2.62E-02 | 2.32E-01 | 4.32E-02 | **9.83E-01** |
|  | Von Neumann | 2.50E-01 | 5.40E-02 | 2.23E-01 | 2.62E-02 | 2.33E-01 | 4.25E-02 | 9.80E-01 |
| f2 | Star | 2.35E-02 | 2.32E-02 | 1.70E-02 | 1.89E-02 | **1.86E-02** | 2.23E-02 | 9.86E-01 |
|  | Ring | 2.39E-02 | 2.67E-02 | 1.70E-02 | 1.89E-02 | 1.84E-02 | 2.23E-02 | 9.87E-01 |
|  | Von Neumann | 2.39E-02 | 2.67E-02 | 1.70E-02 | 1.89E-02 | 1.85E-02 | 2.22E-02 | **9.88E-01** |
| f3 | Star | 1.01E-01 | 2.82E-02 | 1.01E-01 | 2.82E-02 | **9.32E-02** | 2.09E-02 | 9.66E-01 |
|  | Ring | 1.01E-01 | 2.82E-02 | 1.01E-01 | 2.82E-02 | 9.27E-02 | 2.12E-02 | **9.77E-01** |
|  | Von Neumann | 1.01E-01 | 2.82E-02 | 1.01E-01 | 2.82E-02 | 9.30E-02 | 2.11E-02 | 9.69E-01 |
| f4 | Star | 9.62E-02 | 2.99E-02 | 7.81E-02 | 1.45E-02 | **8.68E-02** | 2.23E-02 | 9.87E-01 |
|  | Ring | 9.51E-02 | 3.13E-02 | 7.81E-02 | 1.45E-02 | 8.62E-02 | 2.26E-02 | **9.93E-01** |
|  | Von Neumann | 9.87E-02 | 3.06E-02 | 7.81E-02 | 1.45E-02 | 8.66E-02 | 2.24E-02 | 9.83E-01 |
| f5 | Star | 1.55E-01 | 2.72E-02 | 1.55E-01 | 2.72E-02 | 1.37E-01 | 2.33E-02 | **9.96E-01** |
|  | Ring | 1.55E-01 | 2.72E-02 | 1.55E-01 | 2.72E-02 | **1.38E-01** | 2.26E-02 | 9.94E-01 |
|  | Von Neumann | 1.55E-01 | 2.72E-02 | 1.55E-01 | 2.72E-02 | 1.37E-01 | 2.32E-02 | 9.90E-01 |
| f6 | Star | 1.41E-01 | 3.49E-02 | 1.38E-01 | 2.33E-02 | **1.33E-01** | 2.85E-02 | 9.79E-01 |
|  | Ring | 1.38E-01 | 2.33E-02 | 1.38E-01 | 2.33E-02 | 1.31E-01 | 2.92E-02 | **9.94E-01** |
|  | Von Neumann | 1.44E-01 | 3.46E-02 | 1.38E-01 | 2.33E-02 | 1.32E-01 | 2.89E-02 | 9.78E-01 |
| f7 | Star | 1.92E-01 | 3.16E-02 | 1.78E-01 | 4.26E-02 | **1.84E-01** | 3.81E-02 | 9.64E-01 |
|  | Ring | 1.91E-01 | 4.60E-02 | 1.78E-01 | 4.26E-02 | 1.83E-01 | 3.81E-02 | 9.80E-01 |
|  | Von Neumann | 1.91E-01 | 4.60E-02 | 1.78E-01 | 4.26E-02 | 1.83E-01 | 3.80E-02 | **9.82E-01** |
| f8 | Star | 1.46E-01 | 4.30E-02 | 1.33E-01 | 5.85E-02 | 1.34E-01 | 4.82E-02 | 9.69E-01 |
|  | Ring | 1.42E-01 | 4.32E-02 | 1.33E-01 | 5.85E-02 | 1.34E-01 | 4.80E-02 | **9.84E-01** |
|  | Von Neumann | 1.44E-01 | 3.82E-02 | 1.33E-01 | 5.85E-02 | 1.34E-01 | 4.82E-02 | 9.77E-01 |
| f9 | Star | 1.63E-01 | 3.81E-02 | 1.63E-01 | 3.81E-02 | 1.43E-01 | 4.74E-02 | 9.54E-01 |
|  | Ring | 1.63E-01 | 3.81E-02 | 1.63E-01 | 3.81E-02 | 1.42E-01 | 4.74E-02 | **9.88E-01** |
|  | Von Neumann | 1.63E-01 | 3.81E-02 | 1.63E-01 | 3.81E-02 | 1.43E-01 | 4.88E-02 | 9.63E-01 |
| f10 | Star | 2.36E-02 | 3.04E-02 | 2.36E-02 | 3.04E-02 | **1.60E-02** | 1.85E-02 | 9.61E-01 |
|  | Ring | 2.36E-02 | 3.04E-02 | 2.36E-02 | 3.04E-02 | 1.54E-02 | 1.83E-02 | **9.82E-01** |
|  | Von Neumann | 2.36E-02 | 3.04E-02 | 2.36E-02 | 3.04E-02 | 1.57E-02 | 1.85E-02 | 9.54E-01 |
| f11 | Star | 6.00E-02 | 4.22E-02 | 6.00E-02 | 4.22E-02 | 6.00E-02 | 4.01E-02 | 9.80E-01 |
|  | Ring | 6.00E-02 | 4.22E-02 | 6.00E-02 | 4.22E-02 | 6.00E-02 | 4.01E-02 | 9.80E-01 |
|  | Von Neumann | 5.90E-02 | 4.22E-02 | 6.00E-02 | 4.22E-02 | 6.00E-02 | 4.01E-02 | 9.77E-01 |
| f12 | Star | 1.73E-02 | 1.78E-02 | 1.53E-02 | 1.28E-02 | 1.35E-02 | 1.31E-02 | 9.43E-01 |
|  | Ring | 1.62E-02 | 1.30E-02 | 1.44E-02 | 1.25E-02 | 1.35E-02 | 1.26E-02 | **9.91E-01** |
|  | Von Neumann | 1.84E-02 | 1.53E-02 | 1.84E-02 | 1.53E-02 | **1.36E-01** | 1.28E-02 | 9.58E-01 |

topology offers a balanced trade-off between exploration and exploitation, while Star accelerates convergence but may cause early stagnation. Future directions include dynamic hyperparameter tuning, scaling to higher dimensions, and applying the framework to evolving neural networks and high-stakes domains like cybersecurity. Additionally, we plan to extend the IOHxplainer framework to study evolving neural networks, focusing on reducing their structural complexity while maintaining performance.

## Data availability:

https://github.com/GitNitin02/ioh_pso

## Acknowledgment

## References

[1] Suyog Chandramouli, Yifan Zhu, and Antti Oulasvirta. 2023. Interactive Personalization of Classifiers for Explainability using Multi-Objective Bayesian Optimization. In *Proceedings of the 31st ACM Conference on User Modeling, Adaptation and Personalization*. 34–45.

[2] Rudresh Dwivedi, Devam Dave, Het Naik, Smiti Singhal, Rana Omer, Pankesh Patel, Bin Qian, Zhenyu Wen, Tejal Shah, Graham Morgan, et al. 2023. Explainable AI (XAI): Core ideas, techniques, and solutions. *Comput. Surveys* 55, 9 (2023), 1–33.

[3] A García-Holgado, Andrea Vazquez-Ingelmo, and FJ García-Peñalvo. 2023. Explainable Rules and Heuristics in AI Algorithm Recommendation Approaches—A Systematic Literature Review and Mapping Study. (2023).

[4] Nikolaus Hansen, Anne Auger, Dimo Brockhoff, and Tea Tušar. 2022. Anytime performance assessment in blackbox optimization benchmarking. *IEEE Transactions on Evolutionary Computation* 26, 6 (2022), 1293–1305.

[5] Nikolaus Hansen, Steffen Finck, Raymond Ros, and Anne Auger. 2009. *Real-parameter black-box optimization benchmarking 2009: Noiseless functions definitions*. Ph. D. Dissertation. INRIA.

[6] Essam H Houssein, Ahmed G Gad, Kashif Hussain, and Ponnuthurai Nagaratnam Suganthan. 2021. Major advances in particle swarm optimization: theory, analysis, and application. *Swarm and Evolutionary Computation* 63 (2021), 100868.

[7] James Kennedy and Russell Eberhart. 1995. A new optimizer using particle swarm theory. In *Proceedings of the sixth international symposium on micro machine and human science*, Vol. 3943. Nagoya, Japan: IEEE.

[8] Marius Lindauer, Katharina Eggensperger, Matthias Feurer, André Biedenkapp, Joshua Marben, Philipp Müller, and Frank Hutter. 2019. Boah: A tool suite for multi-fidelity bayesian optimization & analysis of hyperparameters. *arXiv preprint arXiv:1908.06756* (2019).

[9] Qunfeng Liu, Wenhong Wei, Huaqiang Yuan, Zhi-Hui Zhan, and Yun Li. 2016. Topology selection for particle swarm optimization. *Information Sciences* 363 (2016), 154–173.

[10] Scott M Lundberg, Gabriel Erion, Hugh Chen, Alex DeGrave, Jordan M Prutkin, Bala Nair, Ronit Katz, Jonathan Himmelfarb, Nisha Bansal, and Su-In Lee. 2020. From local explanations to global understanding with explainable AI for trees. *Nature machine intelligence* 2, 1 (2020), 56–67.

[11] Nandar Lynn, Mostafa Z Ali, and Ponnuthurai Nagaratnam Suganthan. 2018. Population topologies for particle swarm optimization and differential evolution. *Swarm and evolutionary computation* 39 (2018), 24–35.

[12] Vladimiro Miranda, Hrvoje Keko, and Alvaro Jaramillo Junior. 2008. Stochastic star communication topology in evolutionary particle swarms (EPSO). (2008).

[13] Qingjian Ni and Jianming Deng. 2013. A new logistic dynamic particle swarm optimization algorithm based on random topology. *The Scientific World Journal* 2013, 1 (2013), 409167.

[14] Youwei Sun and Chaoli Sun. 2023. Particle Swarm Optimization with Ring Topology for Multi-modal Multi-objective Problems. In *Proceedings of the Genetic and Evolutionary Computation Conference*. 93–101.

[15] John Von Neumann. 1935. On complete topological spaces. *Trans. Amer. Math. Soc.* 37, 1 (1935), 1–20.